

Knowledge Distillation in Generations: More Tolerant Teachers Educate Better Students

Chenglin Yang
chenglin.yangw@gmail.com

Lingxi Xie
198808xc@gmail.com

Siyuan Qiao
siyuan.qiao@jhu.edu

Alan Yuille
alan.l.yuille@gmail.com

Department of Computer Science
The Johns Hopkins University
Baltimore, 21218 MD, USA

Abstract

This paper studies teacher-student optimization on neural networks, *i.e.*, adopting the supervision from a trained (teacher) network to optimize another (student) network. Conventional approaches enforced the student to learn from a *strict* teacher which fit a hard distribution and achieved high recognition accuracy, but we argue that a more *tolerant* teacher often educate better students.

We start with adding an extra loss term to a *patriarch* network so that it preserves confidence scores on a *primary* class (the ground-truth) and several visually-similar *secondary* classes. The patriarch is also known as the first teacher. In each of the following generations, a student learns from the teacher and becomes the new teacher in the next generation. Although the patriarch is less powerful due to ambiguity, the students enjoy a persistent ability growth as we gradually fine-tune them to fit one-hot distributions. We investigate standard image classification tasks (CIFAR100 and ILSVRC2012). Experiments with different network architectures verify the superiority of our approach, either using a single model or an ensemble of models.

1 Introduction

- “*Indigo comes from blue, but it is bluer than blue.*”
- “*Teachers need not to be wiser than students.*”

—OLD PROVERBS

Deep learning, especially the convolutional neural networks, has been widely applied to computer vision problems. Among them, image classification has been considered the fundamental task which sets the backbone of a vision system [18][26][28][10], and the knowledge or features extracted from these modules can be transferred for generic image representation purposes [23] or other vision tasks [9][24][35][21].

Therefore, in computer vision, a fundamental task is to optimize deep networks for image classification. Most existing works achieved this goal by fitting *one-hot vectors*. For each training sample (\mathbf{x}_n, y_n) where \mathbf{x}_n is an image matrix and y_n is the class label out of C classes, the goal is to find network parameters θ , so that $\mathbf{f}(\mathbf{x}_n; \theta) \approx [0, \dots, 1, \dots, 0]^T$, *i.e.*,

only the y_n -th dimension is 1 and all others are 0. Despite its effectiveness, we argue that this setting forces the image to be classified as the *primary* class (*i.e.*, the ground-truth) with the confidence score of the target class being 1 and others being 0. However, this is not necessarily the optimal fitting target, because allowing for some *secondary* classes (*i.e.*, those that are visually similar to the ground-truth) to be preserved may help to alleviate the risk of over-fitting. Previously, some approaches dealt with this issue by learning a class-level similarity matrix [9][30][63]; but they are unable to capture the image-level similarities, *e.g.*, different *cat* images may be visually similar to different classes.

An alternative solution is to distill knowledge from a trained (*teacher*) network and guide another (*student*) network in order to model the visual similarity [24]. This involves training $G + 1$ models in total, denoted by $\mathbb{M}^{(0)}, \mathbb{M}^{(1)}, \dots, \mathbb{M}^{(G)}$, respectively. $\mathbb{M}^{(0)}$ is named the *patriarch* network, or the first *teacher* network. In each of the following G generations, $\mathbb{M}^{(g)}$ plays the role of the *student* and learns from $\mathbb{M}^{(g-1)}$. Mathematically, each loss function is composed of two terms, *i.e.*, $\mathcal{L}^{(g)} = (1 - \lambda) \cdot \mathcal{L}_C^{(g)} + \lambda \cdot \mathcal{L}_S^{(g)}$. The first term, $\mathcal{L}_C^{(g)}$, is the classification loss (the standard cross-entropy loss), which requires the network to learn visual features that align with the final goal. The second term, $\mathcal{L}_S^{(g)}$, is the similarity loss facilitating the student to learn from the visual knowledge of its teacher. The patriarch does not have a teacher, and so we define a different $\mathcal{L}_C^{(0)}$ accordingly and discard $\mathcal{L}_S^{(0)}$.

This work reveals an interesting phenomenon, that a more tolerant teacher (*i.e.*, a model which tends to distribute the confidence score out of the primary class) often educates better students, because it provides a larger room for the student to capture image-level visual similarity. To this end, we intentionally train $\mathbb{M}^{(0)}$ to fit a softened class distribution, *e.g.*, the primary class has a score of 0.6, and the remaining 0.4 is distributed among a few secondary classes, with the set of secondary classes varying from sample to sample. As the number of generation goes up, the trained model gradually converges to fit the original one-hot distribution, but in comparison to the standard training, our approach produces stronger models. We perform experiments on the CIFAR100 and ILSVRC2012 datasets. Although our approach requires a longer training stage, the testing complexity remains the same, with classification accuracy being much higher, either for single models or model ensemble.

The remainder of this paper is organized as follows. Section 2 briefly reviews related work, and Section 3 describes our approach. After experiments are shown in Section 4, we conclude this work in Section 5.

2 Related Work

Deep learning has been dominating the field of computer vision. Powered by large-scale image datasets [9] and powerful computational resources, it is possible to train very deep networks for various computer vision tasks. The fundamental idea of deep learning is to design a hierarchical structure containing multiple *layers*, each of which contains a number of *neurons* having the same or similar mathematical functions. People believe that a sufficiently deep network is able to fit very complicated distributions in the feature space. In a fundamental task known as image classification, deep neural networks [24] have achieved much higher accuracy than conventional handcrafted features [22]. It is well acknowledged that deeper network structures lead to better performance [26][28][10][15][13], but we still need specifically designed techniques to assist optimization, such as ReLU activation [20], Dropout [27] and batch normalization [16]. People also studied automatic ways of designing

neural network architectures [62][39].

The rapid progress of deep learning has helped a lot of computer vision tasks. Features extracted from trained classification networks can be transferred to small datasets for image classification [6], retrieval [23] or object detection [9]. An even more effective way is to insert specified network modules for these tasks, and initializing these models with part of the weights learned for image classification. This flowchart, often referred to as fine-tuning, works well in a variety of problems, including object detection[8][24], semantic segmentation [19][2], edge detection [65], *etc.*

Since the trained network is deep (*i.e.*, the mathematical function is very complicated) and the amount of training data is limited, it is often instructive to introduce extra *priors* to constrain the training process and thus prevent over-fitting. A common prior assumes that some classes are visually or semantically similar [9], and adds a class-level similarity matrix to the loss function [30][33], but it is unable to deal with image-level similarity which is well noted in previous research [31][0][36]. Another prior is named knowledge distillation, which allows a *teacher* network to guide the optimization of a *student* network. In [12], it was verified that the student network can be of a smaller size than the teacher network, but achieve similar recognition performance with the help of the teacher. This model was later improved so that multiple teachers were used to provide a better guidance [29]. In a recent work named the born-again network [6], the networks are optimized in generations, in which the next generation was guided by the standard one-hot classification vector as well as the knowledge learned in the previous generation.

3 Our Approach

This section presents our approach. We first introduce a framework organized by *generations* (Section 3.1). Then, we provide empirical analysis on why this framework trains deep networks better (Section 3.2), based on which we propose to set tolerant teachers to educate better students (Section 3.3).

3.1 Framework: Network Training in Generations

We consider a standard network optimization task. Given a model \mathbb{M} which has a mathematical form of $\mathbf{y} = \mathbf{f}(\mathbf{x}; \theta)$, where \mathbf{x} and \mathbf{y} are input and output, and θ denotes learnable parameters (*e.g.*, convolutional weights). Given a training set $\mathcal{D} = \{(\mathbf{x}_1, \mathbf{y}_1), \dots, (\mathbf{x}_N, \mathbf{y}_N)\}$, the goal is to determine the parameter θ that best fits these data.

In practice, a popular optimization flowchart starts with setting all weights as white noise, and then applies a gradient-descent-based algorithm to update them. In this scenario, the complicated network design and the limited number of training samples create a high-dimensional feature space in which only a limited number of data points are observed. As a result, it is likely to find a θ to achieve a high accuracy on the training set (*e.g.*, a 110-layer residual network [10] reports almost 100% training accuracy on CIFAR100), but the testing accuracy is still below satisfaction. This phenomenon, often referred to as over-fitting, limits us from generalizing the trained model from training data to unobserved testing data.

We suggest to regularize the training stage with a teacher-student framework¹, in which a *teacher* model $\mathbb{M}^T: \mathbf{f}^T(\mathbf{x}; \theta^T)$ is first trained to capture data distribution, and then used

¹We shall explain why teacher-student training serves as regularization in the next subsection.

to guide a *student model* $\mathbb{M}^S: \mathbf{f}^S(\mathbf{x}; \theta^S)$. We follow [6] to design the loss function. For each training sample $(\mathbf{x}_n, \mathbf{y}_n)$, the loss function $\mathcal{L}(\mathbf{x}_n, \mathbf{y}_n)$ is composed of two terms, *i.e.*, $\mathcal{L} = (1 - \lambda) \cdot \mathcal{L}_C + \lambda \cdot \mathcal{L}_S$, where \mathcal{L}_C and \mathcal{L}_S indicate the **classification loss** and the **similarity loss**, respectively. The classification term is simply the standard cross entropy loss:

$$\mathcal{L}_C(\mathbf{x}_n, \mathbf{y}_n; \mathbb{M}^S) = -\mathbf{y}_n^\top \ln \mathbf{f}^S(\mathbf{x}_n; \theta^S). \quad (1)$$

Since \mathbf{y}_n is a one-hot vector, there is only one term in $\ln \mathbf{y}_n$ being calculated. The similarity loss is the difference between the predicted class distribution \mathbf{f}^S and that of its teacher \mathbf{f}^T , which we measure by computing the KL-divergence:

$$\mathcal{L}_S(\mathbf{x}_n, \mathbf{y}_n; \mathbb{M}^S, \mathbb{M}^T) = \text{KL}[\mathbf{f}^T \parallel \mathbf{f}^S] = -[\mathbf{f}^T]^\top \ln \{\mathbf{f}^S / \mathbf{f}^T\}. \quad (2)$$

Note that \mathbf{f}^S is normalized, *i.e.*, $\|\mathbf{f}^S\|_1 = 1$. In [6], this model was further extended to multi-generation learning. Let there be G generations in total. The *patriarch* model, denoted by $\mathbb{M}^{(0)}$, is the first one to be trained (no teacher is available). In this case, the similarity loss term is discarded, *i.e.*, $\mathbb{M}^{(0)}$ follows a standard training stage with cross-entropy loss. Then in each generation $g = 1, 2, \dots, G$, the student $\mathbb{M}^{(g-1)}$ learns from its teacher $\mathbb{M}^{(g)}$. Finally, $\mathbb{M}^{(G)}$ is more powerful than $\mathbb{M}^{(0)}$ and the ensemble of these models also obtains higher accuracy than that of the same number of standard individual models.

3.2 Analysis: Why Teacher-Student Optimization Works?

Before continuing, we study the reason why teacher-student optimization works better. Traditional literatures referred to this approach by *knowledge distillation*, which is able to (i) train a student network being more compact than the teacher but achieving comparable performance [10]; or (ii) train a student network having the same number of parameters but outperforming the teacher [6]. It was believed that the student can benefit from the knowledge learned by the teacher, but we provide an alternative analysis on what the benefit is, which also inspires our algorithm.

We first note that the difference lies in the term $\text{KL}[\mathbf{f}^T \parallel \mathbf{f}^S]$, where \mathbf{f}^T is the teacher signal, or more precisely, its “prediction” in a training sample. If the teacher is perfectly correct, *i.e.*, \mathbf{f}^T is a one-hot vector with 1 appearing at the ground-truth class, $\text{KL}[\mathbf{f}^T \parallel \mathbf{f}^S]$ is equivalent to the cross-entropy loss and nothing different happens. So, we conjecture that **the teacher network does not produce perfect prediction even in an observed sample**.

We verify this by an empirical study on the CIFAR datasets [10]. A 110-layer residual network [10] is trained, and validated directly in the training data. From Figure 1, we observe three important facts. First, training accuracy is close to 100%, with a dominant amount of confidence (99.8% on CIFAR10 and 98.4% on CIFAR100) at the correct class, but there still exists a little portion of scores assigned to other classes. Second, for each *primary* class, the *secondary* classes sharing a considerable amount of confidence are often semantically similar to it, *e.g.*, in CIFAR10, *cat* is close to *dog*, *automobile* is close to *truck*, *etc.* Third, although semantic similarity exists in the class level, there are still some situations when an image is visually similar to other classes, *e.g.*, *automobile* is most similar to *truck* in 60% of time, but in another 19% and 7% of time, it is most similar to *ship* and *airplane*, respectively. **This is why teacher-student optimization works.** The teacher network learns image-level similarity and allows the student network to preserve such similarity. Without it, the student network needs to fit a one-hot vector, which assumes that all classes have zero similarity with each other, and inevitably results in over-fitting.

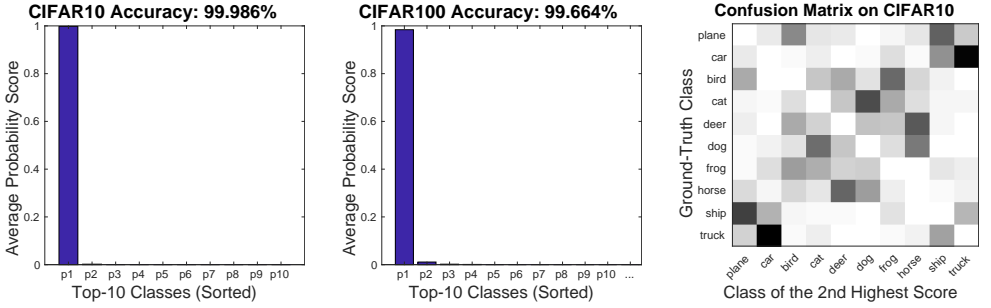


Figure 1: Left: score distributions of a 20-layer ResNet in the *training* sets of CIFAR10 and CIFAR100, in which classes are sorted by their confidence scores in each training sample. Right: the confusion matrix on the *training* set of CIFAR10, and the cell in the i -th row, j -th column indicates the number of training samples of the i -th class in which the **second** highest confidence score appears at the j -th class. The classification accuracy in the CIFAR10/100 *training* sets are 99.986% and 99.664%, respectively.

Despite the usefulness of image-level similarity, existing approaches [14][6] often optimize the teacher network with standard cross-entropy loss in only a small amount of similarity is preserved (see Figure 1). Consequently, the benefit of teacher-student optimization is reduced. In the following, we will modify the loss function of the teacher model, leading to more “tolerant” teachers which have a greater potential to educate better students.

3.3 More Tolerant Teachers, Better Students

Intuitively, we refer to the model with a larger amount of image-level similarity as a model containing higher *energy*. We make two modifications beyond the baseline algorithm: (i) we change the loss function of the patriarch model $\mathbb{M}^{(0)}$ to intentionally create a higher energy level; (ii) we increase the weight of the teacher signal so that the energy does not decay very fast throughout generations.

The definition of $\mathcal{L}^{(0)}$ starts with a hyper-parameter K which is the approximate number of classes that is visually similar to each primary class (including itself). For each input \mathbf{x}_n , these K classes are determined by the classification scores $\mathbf{f}^{(0)}$. We denote the k -th largest dimension in $\mathbf{f}^{(0)}$ by $a_k^{(0)}(\mathbf{x}_n)$ or simply a_k . a_1 is called the primary class, and a_2, \dots, a_K are called the secondary classes. The idea is to constrain the difference between the primary score $f_{a_1}^{(0)}(\mathbf{x}_n)$, or abbreviated as $f_{a_1}^{(0)}$, and the secondary scores $f_{a_k}^{(0)}$, for $k = 2, \dots, K$. Therefore, we add a so-called **score difference term** to the loss function, yielding the updated loss function:

$$\mathcal{L}_C^{(0)}(\mathbf{x}_n, \mathbf{y}_n; \mathbb{M}^{(0)}) = -(1 - \eta) \cdot \mathbf{y}_n^\top \ln \mathbf{f}^{(0)} + \eta \cdot \left[f_{a_1}^{(0)} - \frac{1}{K-1} \sum_{k=2}^K f_{a_k}^{(0)} \right]. \quad (3)$$

Here, η is a hyper-parameter controlling the balance between the ground-truth supervision and the score difference term. Eqn (3) raises a tradeoff between perfect classification ($\mathbf{f}^{(0)}$ is the same as \mathbf{y}_n , i.e., $f_{a_1}^{(0)} = 1$) and sufficient energy ($f_{a_1}^{(0)}$ is not very close to 1). Mathematically, the optimal $\mathbf{f}^{(0)}$ to minimize $\mathcal{L}_C^{(0)}$ shall satisfy $0 < f_{a_1}^{(0)} < 1$, $f_{a_2}^{(0)} + \dots + f_{a_K}^{(0)} = 1 - f_{a_1}^{(0)}$,

and all other entries are 0. We can easily derive the optimal $f_{a_1}^{(0)} \doteq u(\eta)$ which is a monotonically descending function with respect to η .

Two side notes are made on Eqn (3) and hyper-parameter K . First, our formulation does not guarantee the primary class a_1 corresponds to the true class. But as we shall see in experiments, after a sufficient number of training epochs, the training accuracy is always close to 100%. Second, K is often difficult to estimate, and may vary among different primary classes. In practice, we set $K = 5$ for CIFAR100 and ILSVRC2012, because (i) CIFAR100 contains 20 coarse groups and each of them has 5 finer-level classes; and (ii) an important evaluation metric on ILSVRC2012 is top-5 accuracy – which is an approximate estimation of K . Of course, fixing K for all classes is very rough, but we shall see in experiments that this simple formulation indeed works.

At the g -th generation, *i.e.*, $\mathbb{M}^{(g)}$ learns from $\mathbb{M}^{(g-1)}$, we use the same loss function described in Section 3.1, namely

$$\mathcal{L}^{(g)}(\mathbf{x}_n, \mathbf{y}_n; \mathbb{M}^{(g)}, \mathbb{M}^{(g-1)}) = -(1 - \lambda) \cdot \mathbf{y}_n^\top \ln \mathbf{f}^{(g)} - \lambda \cdot [\mathbf{f}^{(g-1)}]^\top \ln \left\{ \mathbf{f}^{(g)} / \mathbf{f}^{(g-1)} \right\}, \quad (4)$$

where λ is another hyper-parameter controlling the the balance between the supervisions from the ground-truth and the teacher signal. Mathematically, the optimal $\mathbf{f}^{(g)}$ to minimize $\mathcal{L}^{(g)}$ shall satisfy $0 < f_{a_1}^{(g)} < 1$, $f_{a_2}^{(g)} + \dots + f_{a_K}^{(g)} = (1 - f_{a_1}^{(g)})$, and all other entries are 0, just like $\mathbf{f}^{(0)}$. Similarly, we have $f_{a_1}^{(g)} \doteq w(\lambda, \mathbf{f}^{(g-1)})$ which is monotonically descending with respect to λ . Therefore, the multi-generation optimization process is parameterized by K , η and λ . We fix K to be 5, and use $f_{a_1}^{(0)} = u(\eta)$ to equivalently replace η , so that each process is denoted by $\mathcal{D}(f_{a_1}^{(0)}, \lambda)$. As examples, training individual models corresponds to $\mathcal{D}(1.0, 0.0)$, and training born-again networks [B] corresponds to $\mathcal{D}(1.0, 0.5)$.

Regardless of $f_{a_1}^{(g)}$ and λ , as $g \rightarrow +\infty$, $f_{a_1}^{(g)} \rightarrow 1$ and so the optimal $\mathbf{f}^{(g)}$ gradually converges to the ground-truth one-hot vector, but as we shall see in experiments, setting a small $f_{a_1}^{(0)}$ and a large λ boosts the energy during the training process, and leads to better models. This phenomenon can also be explained using the simulated annealing theory. Using a smaller $f_{a_1}^{(0)}$ is similar to setting a higher temperature in the annealing process (the patriarch model often reports a lower accuracy). A smaller λ allows the ambiguity to decrease gradually, corresponding to setting a lower annealing rate which brings higher stability (the students enjoy a persistent accuracy gain and eventually outperform the baseline).

4 Experiments

4.1 The CIFAR100 Dataset

- **Settings and Baselines**

We first evaluate our approach on the CIFAR100 dataset [B], which contains 60,000 tiny RGB images of a spatial resolution of 32×32 . These images are split into a training set of 60,000 samples and a testing set of 10,000 samples. Both training and testing images are uniformly distributed over 100 classes. Note that we do not experiment on the CIFAR10 dataset because the number of classes are too small to reveal the effectiveness of our gradual optimization strategy.

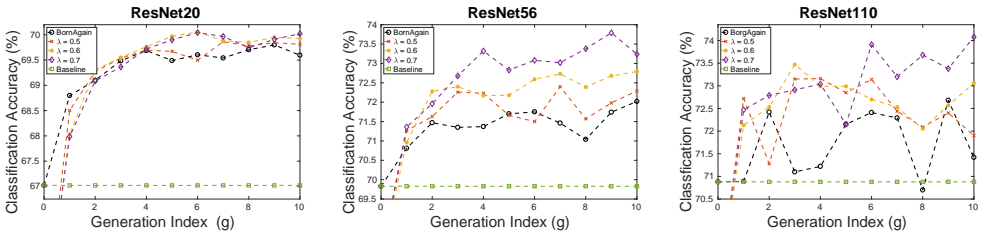


Figure 2: Classification accuracy produced by different hyper-parameters in $\mathcal{D}(f_{a_1}^{(0)}, \lambda)$. The “Baseline” is $\mathcal{D}(1.0, 0.0)$, “BornAgain” is $\mathcal{D}(1.0, 0.5)$, and for the others, we fix $f_{a_1}^{(0)} = 0.6$. The dashed line in each sub-plot indicates the baseline accuracy.

We start with the deep residual networks (ResNets) [14] with different layers, *i.e.*, $L \in \{20, 32, 44, 56, 74, 92, 110\}$, or $L = 6L' + 2$ layers where L' is an integer. The first 3×3 convolutional layer is first performed on the 32×32 input image without changing its spatial resolution, then three stages followed, each of which has L' residual blocks (two 3×3 convolutions plus one identity connection). Batch normalization [16] and ReLU activation [20] are added after each convolution. The spatial resolution of the input remain unchanged in the three stages (32×32 , 16×16 and 8×8), and the number of channels are 16, 32 and 64, respectively. Average pooling layers are inserted after the first two stages for down-sampling. The network ends with a fully-connected layer with 100 outputs.

Our approach is also experimented on the densely connected convolutional networks (DenseNets) [15] with 100 and 190 layers. The overall architecture is similar to the ResNets, but the building blocks are densely-connected, *i.e.*, each basic unit takes the input feature, convolves it twice, and concatenates it to the original feature. We use the 100-layer DenseNet with a base number of channels of 24 and a growth rate of 12.

We follow the conventions to train these networks from scratch. We use the standard Stochastic Gradient Descent (SGD) with a weight decay of 0.0001 and a Nesterov momentum of 0.9. In the ResNets, we train the network for 164 epochs with mini-batch size of 128. The base learning rate is 0.1, and is divided by 10 after 82 and 123 epochs. In the DenseNets, we train the network for 300 epochs with a mini-batch size of 64. The base learning rate is 0.1, and is divided by 10 after 150 and 225 epochs. In the training process, the standard data-augmentation is used, *i.e.*, each image is padded with a 4-pixel margin on each of the four sides. In the enlarged 40×40 image, a subregion with 32×32 pixels is randomly cropped and flipped with a probability of 0.5. No augmentation is used at the testing stage.

• Results

We first evaluate the performance with respect to different hyper-parameters, namely, different parameterized processes $\mathcal{D}(f_{a_1}^{(0)}, \lambda)$. We fix $K = 5$ and $f_{a_1}^{(0)} = 0.6$, and diagnose the impact of λ on deep residual networks [14] with different numbers of layers. We also evaluate the born-again networks [5] which corresponds to $\mathcal{D}(1.0, 0.5)$.

Results are summarized in Figure 1. We can observe several important properties of our algorithm. First, a strict teacher (*i.e.*, the born-again network [5], $\mathcal{D}(1.0, 0.5)$) is inferior to a tolerant teacher (*e.g.*, $\mathcal{D}(0.6, 0.5)$). Although the latter often starts with a lower accuracy of the patriarch model, it has the ability of gradually and persistently growing up and outperforming the baseline after 1–3 generations. It is possible to see the accuracy saturate after

	Gen #0	Gen #1	Gen #2	Gen #3	Gen #4	Gen #5
Baseline (100 layers)	22.88	–	–	–	–	–
$\mathcal{D}(0.6, 0.6)$	23.96	21.29	20.51	20.83	21.01	21.27
+Ensemble	–	20.22	18.29	17.62	17.32	17.05
$\mathcal{D}(0.6, 0.7)$	23.96	21.72	20.77	21.02	21.47	21.61
+Ensemble	–	20.57	19.19	18.63	17.94	17.42
Baseline (190 layers)	17.17	–	–	–	–	–
$\mathcal{D}(0.6, 0.6)$	18.87	17.42	17.26	17.13	17.24	17.01
+Ensemble	–	16.64	16.00	15.41	15.24	15.11
$\mathcal{D}(0.6, 0.7)$	18.87	17.81	17.55	17.51	17.37	17.50
+Ensemble	–	16.91	16.12	15.72	15.15	14.85
	[58]	[14]	[11]	[57]	[7]	[6]
State-of-the-Arts	19.25	17.40	17.01	16.80	15.85	14.90

Table 1: Top-1 and top-5 error rates (%) by different models on CIFAR100. In each group, all networks have the same depth. Gen #0 stands for the patriarch. All the competitors were published in 2017. We use a GitHub repository² as our baseline (the numbers are from this website), but our re-implementation reports slightly worse numbers.

a few generations, because eventually the teacher signal will converge to the points that are dominated by the primary classes (*i.e.*, $f_{a_1}^{(g)} \rightarrow 1$), and the teacher will become strict again. Second, the number of layers impacts the choice of the teaching parameter λ . In a relatively deep network, a large λ (*e.g.*, 0.7) works better than a small λ (*e.g.*, 0.6), while it is the opposite in a relatively shallow network. This is because knowledge distillation requires higher temperature (larger energy) for deeper networks [14]. As a side note, the ensemble of the models in our algorithm (*e.g.*, $\mathcal{D}(0.6, 0.6)$) is considerably better than that of the models trained individually ($\mathcal{D}(1.0, 0.0)$) or from a strict teacher ($\mathcal{D}(1.0, 0.5)$).

In DenseNets with 100 and 190 layers, we report both single-model and model-ensemble results in Table 1. We evaluate $\mathcal{D}(0.6, 0.6)$ and $\mathcal{D}(0.6, 0.7)$, and observe the same phenomena as in ResNet experiments (both single-model and model-ensemble works favorably). In particular, in DenseNet100, our single-model accuracy is 1%–2% higher, and our 5-model ensemble accuracy is more than 5% higher and even outperforms single DenseNet190 models. Considering DenseNet190 requires around $30\times$ FLOPs of DenseNet100, this is quite an efficient method to achieve high classification accuracy. In DenseNet190, our results are competitive to the state-of-the-arts. Note that [57] and [7] applied complicated data augmentation approaches to achieve high accuracy, but we found a different way, which is to improve the optimization algorithm.

We inherit these learned parameters to the large-scale experiments on ILSVRC2012 (the costly computation avoids us from tuning this hyper-parameter). We use $\mathcal{D}(0.6, 0.6)$. As ResNet18 (18 layers, not very deep) is chosen as the baseline.

4.2 The ILSVRC2012 Dataset

• Settings and Baselines

²<https://github.com/bearpaw/pytorch-classification>

	Gen #0		Gen #1		Gen #2		Gen #3		Gen #4		Gen #5	
Baseline	30.50	11.07	–	–	–	–	–	–	–	–	–	–
$\mathcal{D}(0.6, 0.6)$	32.52	11.23	30.28	10.23	30.12	10.15	29.92	10.25	29.77	10.19	29.60	10.11
+Ensemble	–	–	30.01	9.98	28.94	9.53	28.51	9.36	28.23	9.28	28.08	9.23

Table 2: Classification error rates (%) by different models on ILSVRC2012. Gen #0 stands for the patriarch. In each group, we report top-1 and top-5 errors.

With the knowledge and parameters learned from the CIFAR100 experiments, we now investigate the ILSVRC2012 dataset [25], a popular subset of the ImageNet database [3]. There are 1,000 classes in total. The training set and testing set contains 1.3M and 50K high-resolution images, with each class having approximately the same number of training images and exactly the same number of testing images.

We set the 18-layer residual network [14] as our baseline. The 224×224 input image is passed through a 7×7 convolutional layer with a stride of 2, and a 2×2 max-pooling layer. Then four stages followed, each with 2 standard residual blocks (two 3×3 convolution layers plus an identity connection). The spatial resolution of these four stages are 56×56 , 28×28 , 14×14 and 7×7 , and the number of channels are 64, 128, 256 and 512, respectively. Three max-pooling layers are inserted between these four stages. The network ends with a fully-connected layer with 1,000 outputs.

All networks are trained from scratch. We follow [13] in configuring the following parameters. Standard Stochastic Gradient Descent (SGD) with a weight decay of 0.0001 and a Nesterov momentum of 0.9 is used. There are a total of 100 epochs in the training process, and the mini-batch size is 1024. The learning rate starts with 0.6, and is divided by 10 after 30, 60 and 90 epochs. In the training process, we apply a series of data-augmentation techniques, including rescaling and cropping the image, randomly mirroring and rotating (slightly) the image, changing its aspect ratio and performing pixel jittering. In the testing process, we use the standard single-center-crop on each image.

• Results

We still set $K = 5$ and $f_{a_1}^{(0)} = 0.6$. Following CIFAR100 experiments, we use $\lambda = 0.6$. Results are summarized in Table 2. One can observe very similar results as in the previous experiments, *i.e.*, a worse patriarch³, gradual and persistent improvement, and saturation after several generations. Although the performance is not comparable to deeper network structures, the accuracy gain (0.90% top-1 and 0.96% top-5) is higher than other two light-weighted modules, namely Squeeze-and-Excitation (SE) [13] (0.72% top-1 and 0.80% top-5) and Second-Order Response Transform (SORT) [62] (0.55% top-1 and 0.27% top-5). Different from them, our approach does not require any additional computation at the testing stage, although the training stage is longer.

5 Conclusions

In this work, we present an approach for optimizing deep networks. Under the framework of teacher-student optimization, our motivation is to set a tolerant teacher by adding a loss

³It is interesting yet expected that the top-1 accuracy of the patriarch is 1.98% lower than the baseline, but the top-5 accuracy is merely 0.16% lower. This is because setting $K = 5$ hardly impacts top-5 classification.

term measuring the difference among top- K scores. This allows the network to preserve sufficient energy which decays gradually, which fits better the theory of knowledge distillation. Experiments on image classification verify our assumption. With the same network (thus the same computational costs at the testing stage), our model works consistently better.

Our research votes for the opinion that network optimization is far from perfect at the current status. In the future, we will investigate a more generalized model, including using a variable function at each generation and allowing K to be varying from case to case. In addition, we will consider a *temperature* term in Eqn (4) to adjust the KL-divergence. Both are expected to achieve better optimization results.

References

- [1] Z. Akata, F. Perronnin, Z. Harchaoui, and C. Schmid. Label-embedding for image classification. *IEEE Transactions on Pattern Analysis and Machine Intelligence*, 38(7): 1425–1438, 2016.
- [2] L. C. Chen, G. Papandreou, I. Kokkinos, K. Murphy, and A. L. Yuille. Deeplab: Semantic image segmentation with deep convolutional nets, atrous convolution, and fully connected crfs. In *International Conference on Learning Representations*, 2016.
- [3] J. Deng, W. Dong, R. Socher, L.J. Li, K. Li, and L. Fei-Fei. Imagenet: A large-scale hierarchical image database. In *Computer Vision and Pattern Recognition*, 2009.
- [4] J. Deng, A. C. Berg, K. Li, and L. Fei-Fei. What does classifying more than 10,000 image categories tell us? In *European conference on computer vision*, 2010.
- [5] J. Donahue, Y. Jia, O. Vinyals, J. Hoffman, N. Zhang, E. Tzeng, and T. Darrell. Decaf: A deep convolutional activation feature for generic visual recognition. In *International Conference on Machine Learning*, 2014.
- [6] T. Furlanello, Z. C. Lipton, L. Itti, and A. Anandkumar. Born again neural networks. In *NIPS Workshop on Meta Learning*, 2017.
- [7] X. Gastaldi. Shake-shake regularization. *arXiv preprint arXiv:1705.07485*, 2017.
- [8] R. Girshick. Fast r-cnn. In *Computer Vision and Pattern Recognition*, 2015.
- [9] R. Girshick, J. Donahue, T. Darrell, and J. Malik. Rich feature hierarchies for accurate object detection and semantic segmentation. In *Computer Vision and Pattern Recognition*, 2014.
- [10] D. Han, J. Kim, and J. Kim. Deep pyramidal residual networks. In *Computer Vision and Pattern Recognition*, 2017.
- [11] K. He, X. Zhang, S. Ren, and J. Sun. Deep residual learning for image recognition. In *Computer Vision and Pattern Recognition*, 2016.
- [12] G. Hinton, O. Vinyals, and J. Dean. Distilling the knowledge in a neural network. *arXiv preprint arXiv:1503.02531*, 2015.
- [13] J. Hu, L. Shen, and G. Sun. Squeeze-and-excitation networks. In *Computer Vision and Pattern Recognition*, 2018.

- [14] G. Huang, Y. Li, G. Pleiss, Z. Liu, J. E. Hopcroft, and K. Q. Weinberger. Snapshot ensembles: Train 1, get m for free. In *International Conference on Learning Representations*, 2017.
- [15] G. Huang, Z. Liu, K. Q. Weinberger, and L. van der Maaten. Densely connected convolutional networks. In *Computer Vision and Pattern Recognition*, 2017.
- [16] S. Ioffe and C. Szegedy. Batch normalization: Accelerating deep network training by reducing internal covariate shift. In *International Conference on Machine Learning*, 2015.
- [17] A. Krizhevsky and G. Hinton. Learning multiple layers of features from tiny images. 2009.
- [18] A. Krizhevsky, I. Sutskever, and G. E Hinton. Imagenet classification with deep convolutional neural networks. In *Advances in Neural Information Processing Systems*, 2012.
- [19] J. Long, E. Shelhamer, and T. Darrell. Fully convolutional networks for semantic segmentation. In *Computer Vision and Pattern Recognition*, 2015.
- [20] V. Nair and G. E. Hinton. Rectified linear units improve restricted boltzmann machines. In *International Conference on Machine Learning*, 2010.
- [21] A. Newell, K. Yang, and J. Deng. Stacked hourglass networks for human pose estimation. In *European Conference on Computer Vision*, 2016.
- [22] F. Perronnin, J. Sanchez, and T. Mensink. Improving the fisher kernel for large-scale image classification. In *European conference on computer vision*, 2010.
- [23] A. S. Razavian, H. Azizpour, J. Sullivan, and S. Carlsson. Cnn features off-the-shelf: an astounding baseline for recognition. In *Computer Vision and Pattern Recognition*, 2014.
- [24] S. Ren, K. He, R. Girshick, and J. Sun. Faster r-cnn: Towards real-time object detection with region proposal networks. In *Advances in Neural Information Processing Systems*, 2015.
- [25] O. Russakovsky, J. Deng, H. Su, J. Krause, S. Satheesh, S. Ma, Z. Huang, A. Karpathy, A. Khosla, M. Bernstein, et al. Imagenet large scale visual recognition challenge. *International Journal of Computer Vision*, 115(3):211–252, 2015.
- [26] K. Simonyan and A. Zisserman. Very deep convolutional networks for large-scale image recognition. In *International Conference on Learning Representations*, 2015.
- [27] N. Srivastava, G. E. Hinton, A. Krizhevsky, I. Sutskever, and R. Salakhutdinov. Dropout: A simple way to prevent neural networks from overfitting. *Journal of Machine Learning Research*, 15(1):1929–1958, 2014.
- [28] C. Szegedy, W. Liu, Y. Jia, P. Sermanet, S. Reed, D. Anguelov, D. Erhan, V. Vanhoucke, A. Rabinovich, et al. Going deeper with convolutions. In *Computer Vision and Pattern Recognition*, 2015.

- [29] A. Tarvainen and H. Valpola. Mean teachers are better role models: Weight-averaged consistency targets improve semi-supervised deep learning results. In *Advances in Neural Information Processing Systems*, 2017.
- [30] N. Verma, D. Mahajan, S. Sellamanickam, and V. Nair. Learning hierarchical similarity metrics. In *Computer Vision and Pattern Recognition*, 2012.
- [31] J. Wang, T. Leung, C. Rosenberg, J. Wang, J. Philbin, B. Chen, Y. Wu, et al. Learning fine-grained image similarity with deep ranking. In *Computer Vision and Pattern Recognition*, 2014.
- [32] Y. Wang, L. Xie, C. Liu, S. Qiao, Y. Zhang, W. Zhang, Q. Tian, and A. Yuille. Sort: Second-order response transform for visual recognition. In *International Conference on Computer Vision*, 2017.
- [33] C. Wu, M. Tygert, and Y. LeCun. Hierarchical loss for classification. *arXiv preprint arXiv:1709.01062*, 2017.
- [34] L. Xie and A. Yuille. Genetic cnn. In *International Conference on Computer Vision*, 2017.
- [35] S. Xie and Z. Tu. Holistically-nested edge detection. In *International Conference on Computer Vision*, 2015.
- [36] C. Zhang, J. Cheng, and Q. Tian. Image-level classification by hierarchical structure learning with visual and semantic similarities. *Information Sciences*, 422:271–281, 2018.
- [37] H. Zhang, M. Cisse, Y. N. Dauphin, and D. Lopez-Paz. mixup: Beyond empirical risk minimization. *arXiv preprint arXiv:1710.09412*, 2017.
- [38] T. Zhang, G. J. Qi, B. Xiao, and J. Wang. Interleaved group convolutions. In *Computer Vision and Pattern Recognition*, 2017.
- [39] B. Zoph and Q. V. Le. Neural architecture search with reinforcement learning. In *International Conference on Learning Representations*, 2017.